Responses of hydropower generation and sustainability to changes in reservoir policy, climate and land use under uncertainty

A case study of Xinanjiang Reservoir in China

Guo, Yuxue; Fang, Guohua; Xu, Yue Ping; Tian, Xin; Xie, Jingkai

DOI
10.1016/j.jclepro.2020.124609

Publication date
2021

Document Version
Final published version

Published in
Journal of Cleaner Production

Journal of Cleaner Production 281 (2021) 124609

Contents lists available at ScienceDirect

Journal of Cleaner Production

journal homepage: www.elsevier.com/locate/jclepro

Responses of hydropower generation and sustainability to changes in reservoir policy, climate and land use under uncertainty: A case study of Xinanjiang Reservoir in China

Yuxue Guo [a], Guohua Fang [b], Yue-Ping Xu [a, *], Xin Tian [c, d], Jingkai Xie [a]

[a] Institute of Hydrology and Water Resources, Civil Engineering and Architecture, Zhejiang University, Hangzhou, 310058, China
[b] College of Water Conservancy and Hydropower Engineering, Hohai University, Nanjing, 210098, China
[c] KWR Water Research Institute, Groningenhaven 7, 3433 PE, Nieuwegein, The Netherlands
[d] Department of Water Management, Delft University of Technology, Stevinweg 1, 2628 CN, Delft, The Netherlands

A R T I C L E I N F O

Article history:
Received 20 October 2019
Received in revised form
7 August 2020
Accepted 9 October 2020
Available online 12 October 2020

Handling editor Yutao Wang

Keywords:
Hydropower generation
Sustainability
Climate and land use change
Reservoir policy
Robust optimization

A B S T R A C T

Climate and land use changes will affect the hydrological regime, and therefore hydropower. This study which aims to develop a novel modeling framework, does not only determine the changes in hydropower generation and sustainability, but also provide robust operating rules for handling uncertainty attributed to both climate and land use changes, using Xinanjiang Reservoir in Eastern China as a case study. Specifically, projections of five bias-corrected and downscaled General Circulation Models (GCMs) and three modeled land uses representing a range of tradeoffs between ecological protection and urban development are employed to drive the Soil and Water Assessment Tool (SWAT) and to predict streamflow under 15 scenarios. We then develop a set of robust rule curves to consider the potential uncertainty in reservoir inflow and to increase hydropower generation, and a baseline rule is presented for comparison. Results show that both robust and baseline rules increase hydropower generation with increasing reservoir inflows in future, but the robust rule yields better hydropower generation, sustainability and efficiency. The streamflow under the rapid urbanization scenarios differs from that under other scenarios, but there are no significant differences in hydropower among scenarios corresponding to the non-linear relationship between streamflow and hydropower change. Our findings highlight the potential to improve water resource utilization in the future, especially based on the robust operating rule considering optimization and uncertainty, and can provide references for future hydropower planning to the other existing plants.

1. Introduction

Renewable hydropower plays a key role in human lives and economic development (Teotónio et al., 2017). According to the 2019 Hydropower Status Report, the world's hydropower has been steadily developing with an increased hydropower capacity of 21.8 GW in 2018, and the total installed capacity reached 1,292 GW. To date, China's hydropower sector has covered over a quarter of the world's installed capacity. It is well known that China has been planning and implementing a number of hydropower plants with reservoirs in different regions, such as the Xinanjiang Reservoir (Vonk et al., 2014) in Qiantangjiang Basin, Three Georges Reservoir (Qin et al., 2019) and Danjiangkou Reservoir (Zhang et al., 2019) in Changjiang Basin, and Xiaolangdi Reservoir (Wang et al., 2016) in Yellow River Basin. These reservoir projects ensure that hydropower remains a vital and stable component of the electricity supply with inherent uncertainty in China.

Hydropower generation can be strongly impacted by hydrological regime, and thus an important issue being discussed recently is how hydropower changes in the future. Climate and land use changes are the two widely believed factors profoundly affecting hydrological processes (Alaoui et al., 2014; Ning et al., 2016; Abera et al., 2019), and thus hydropower generation. However, hydropower generation and climate change, or hydropower generation and land use change both have a coupled relationship, and they interact with each other. On one hand, climate change indirectly influences streamflow through variations in

* Corresponding author. .
E-mail address: yuepingxu@zju.edu.cn (Y.-P. Xu).

https://doi.org/10.1016/j.jclepro.2020.124609

temperature, precipitation, and evaporation (Ahn and Merwade, 2014; Guo et al., 2019), and land use change alters variables such as evapotranspiration, groundwater re-charge and overland flow, resulting in changes in streamflow (Molina-Navarro et al., 2014; Zhang et al., 2017). Furthermore, the spatiotemporal variations in streamflow will change the reservoir inflow and thus affect hydropower generation. On the other hand, hydropower is beneficial to reduction in the dependence on fossil fuels and the emissions of greenhouse gas (GHG), and reservoir operation may contribute to mitigating local climate change (De Queiroz et al., 2016); meanwhile, hydropower improves the energy supply security and reliability accelerating economic development and supporting a growing global population, potentially resulting in land use redistribution. Given the significant role of hydropower, to assess the individual and combined climate and land use changes on hydropower generation is critical for sustainable development.

Numerous studies have investigated how climate change impacts streamflow and hydropower generation, and most of them have applied General Circulation Model (GCM) projections to quantify these effects (Schaeffer et al., 2012; Boehlert et al., 2016; Kim et al., 2017; Mendes et al., 2017; Falchetta et al., 2019; Zhong et al., 2019). Turner et al. (2017a, 2017b) explored the possible impacts of climate change on global hydropower by an aggregated hydrological and hydropower plant operating model depending on GCMs; the former found that the majority of hydropower plants experienced reductions in hydropower production under all emissions scenarios, and the latter highlighted the disagreements in the direction of changes in hydropower production at the global scale. Moreover, regional studies conducted in many regions of the world have noted that hydropower generation was projected to increase in some areas and decrease in others under climate change (Chilkoti et al., 2017; Teotónio et al., 2017; Arango-Aramburo et al., 2019; De Queiroz et al., 2019). For example, Mendes et al. (2017) reported that hydropower outputs was reduced with decreasing streamflow in Iberian area by coupling GCMs and a hydrology-reservoir model, while Zhong et al. (2019) followed a similar method to predict future hydropower in the Lancangjiang hydropower base, and noted that increased reservoir inflows would cause increments in hydropower outputs for most GCMs. Additionally, the effects of land use change on hydrological processes have been widely discussed (Zhang et al., 2015; Zuo et al., 2016; Desta et al., 2019). However, to our best knowledge, there has been very limited efforts to review the impacts of land use change, and even fewer studies have focused on the combined impacts of climate and land use changes on hydropower variations.

Accordingly, the most common way to evaluate how future changes impact hydropower generation is by coupling hydrological models with climate or land use models to first simulate the streamflow response and then estimate hydropower generation based on the relevant operation policies that describe the relationship between streamflow and hydropower generation. However, the earlier mentioned studies mainly focused on the assessment of potential hydropower changes based on a power output equation with a constant hydraulic head. They did not consider the use of optimal reservoir policy as well as the ability of operating policy to mitigate the impacts attributed to future uncertain climatic and/or land use changes. The differences in hydropower plant operation policies considering climate and land use changes remain unclear. A number of methods to address uncertainty in reservoir operation have been proposed in recent years (Xu and Tung, 2008, 2009; Kasprzyk et al., 2009; Matrosov et al., 2013; Culley et al., 2016; Beh et al., 2017), one of which is robust optimization. Robust optimization has shifted from expected utility to exploratory bottom-up approaches, which can identify and secure vulnerable scenarios in advance (Giuliani et al., 2014). Managers generally refuse to use the optimization models to directly operate reservoirs, particularly when they consider realistic uncertainties (Celeste and Billib, 2009). They prefer some simpler tools instead, such as rule curves, which are different from the operating solutions informed from the robust optimization analysis (Kasprzyk et al., 2013). Moreover, the former studies generally focused on the overall changes in hydropower production and the resulting economic impacts, whereas the sustainability of the future hydropower systems, including the reliability to maintain base output, and the resiliency and vulnerability to output failure, which can be used to quantify and identify how different reservoir policies response to future changes, is still less investigated.

The Xinanjiang catchment in Eastern China is a good case study given that its power sector is highly dependent on hydropower. The Xinanjiang hydropower plant is the first nationally designed and constructed reservoir in China. Dominated by global warming, rapid urbanization and land use policies in the Xinanjiang catchment, the inflow and hydropower generation of Xinanjiang Reservoir are undergoing dramatic changes. We aim to evaluate the hydropower changes induced by different operating policies, climate and land use changes, using Xinanjiang Reservoir as a case study. The innovations of this study are as follows: (1) The overall changes in the hydropower potential and outputs as well as the sustainability of hydropower projects are assessed under the combined impacts of climate and land use changes; (2) Robust optimization curve is developed to mitigate the impacts attributed to the uncertainty, and a baseline curve is presented for comparisons. Specifically, the projections of bias-corrected GCMs and modeled land uses are employed as inputs of the Soil and Water Assessment Tool (SWAT) to predict streamflow under multiple scenarios. Then the streamflow changes and corresponding information are considered when developing robust reservoir operation rules, and the hydropower generation and sustainability in the future are finally assessed based on the baseline and robust rules.

2. Case study description

2.1. Study area

The Xinanjiang catchment is located in the upstream part of Qiantangjiang Basin, Eastern China. The Xinanjiang River flows from west to east across two provinces in China, namely, Anhui and Zhejiang, and has a total length of 323 km with a drainage area of 11,503 km^2, as shown in Fig. 1. Forest and grassland are the most widely distributed, and cultivated land is concentrated on the periphery of urban land. Located in the subtropical monsoon climate zone, the seasonal temperature and precipitation differences are distinct. Note that the spring and summer account for the most precipitation among the four seasons. The wet seasons from March to July account for approximately 74% of the annual streamflow, and the dry seasons from August to February take up the remaining 26% of streamflow.

The Xinanjiang hydropower plant with reservoir located upstream of the Qiantangjiang Basin (presented in Fig. 1), is mainly utilized for electricity supply for the East China Power Grid including Shanghai city and Jiangsu, Zhejiang and Anhui provinces. The reservoir characteristic parameters are listed in Table 1. Under normal conditions, the Xinanjiang Reservoir operates through a monthly conventional policy (the baseline rule) closely based on the dynamics of the current releases and flows, including different guide curves and the corresponding operation zones for hydropower generation. The baseline rule is between the minimum water level and the maximum water level, within a lower basic guiding curve, an upper basic guiding curve, 1.5-times output and 2-times output curve in detail.

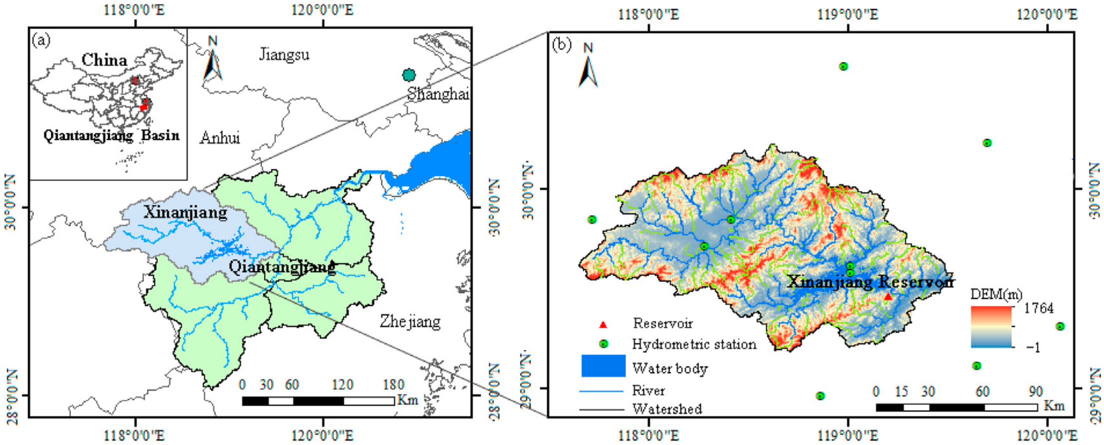

Fig. 1. Geographic location of (a) Qiantangjiang Basin and (b) Xinanjiang catchment.

Table 1
Characteristic parameters of Xinanjiang Reservoir.

Reservoir	Normal water level	Flood limited water level	Dead water level	Power output coefficient	Installed capacity	Firm capacity
	m				MW	
Xinanjiang	108	106.5	86	8.3	810	174

2.2. Data

The data used in this study are described in Table 2. Specifically, the observed meteorological data comprise the daily precipitation, temperature, solar radiation, wind speed, and relative humidity, which are collected at nine hydrometric stations, namely Ningguo, Huangshan, Linan, Qimen, Tunxi, Chunan, Jinhua, Yiwu, and Quzhou, as presented in Fig. 1. The GCM climate projections include the daily precipitation and average, maximum and minimum temperature. Five CMIP5 GCMs, CNRM-CM5, GEDL-ESM2M, IPSL-CM5A-LR, MIORC-ESM-CHEM, and NORESM1-M are used to indicate the inter-model uncertainties due to their good performance in climate simulation and projection in China (Wen et al., 2018; Yang et al., 2019).

3. Methods

We proposed an integrated and systematic framework to assess the potential changes in hydropower generation, sustainability and efficiency induced by reservoir policy, climate and land use change under uncertainty, as presented in Fig. 2. The main methods associated with the framework are described as follows.

3.1. Climate and land use change scenarios

To identify how different climate scenarios impact streamflow, we select three Representative Concentration Pathways (RCP) scenarios, namely RCP2.6, RCP4.5 and RCP8.5, in this study. These three scenarios represent low, medium and high emissions of GHG, respectively. The five GCMs projected precipitation and temperature at daily scale under RCPs will be downscaled and bias-corrected by the Bias Correction and Spatial Disaggregation daily (BCSDd) method (Thrasher et al., 2012). The description of the BCSDd method is reported in the supplemental material.

Additionally, three land use change scenarios that represent a range of tradeoffs between ecological protection and urban development are considered to identify how different land use management policies affect streamflow, and these scenarios include the historical trend (HT), ecological protection (EP), and urban development (UD) scenarios. The land use demands under the three scenarios are all based on the historical trend from 2005 to 2015, but vary with specific conditions. The HT scenario represents the conditions without any interventional policy for land use changes in the future; the EP scenario aims to maintain a high vegetation coverage rate and develop ecological land areas (forest and grassland) to other land use types; and the UD scenario not only forbids the transformation of urban land to other land use types, but also encourages the conversion to urban land. Overall, the EP scenario has a lower impermeable area (IA), but the UD scenario has a greater IA. We used the Cellular Automata - Markov (CA-Markov) model (Wickramasuriya et al., 2009) to predict the land use change in 2025. The description of the CA-Markov model is reported in the supplemental material.

Then, 15 scenarios are assumed to assess the individual and

Table 2
Research data used in this study.

Data types	Research data	Period	Sources
Geospatial data	Digital elevation model (DEM)	2000	Geospatial Data Cloud of China (http://www.gscloud.cn)
	Land use	1995, 2005, 2015	Resource and Environment Data Cloud Platform of China (http://www.resdc.cn)
	Soil	2008	Cold and Arid Regions Sciences Data Center at Lanzhou (http://westdc.westgis.ac.cn)
Meteorological data	Daily observed data	1976–2005	National Meteorological Information Center of China (http://data.cma.cn)
	Daily GCM projections	Baseline: 1976–2005; Future: 2021–2050	Earth System Grid Federation (https://esgf-node.llnl.gov)
Discharge data	Monthly inflow of Xinanjiang Reservoir	1976–2005	Zhejiang Design Institute of Water Conservancy & Hydro-electric Power

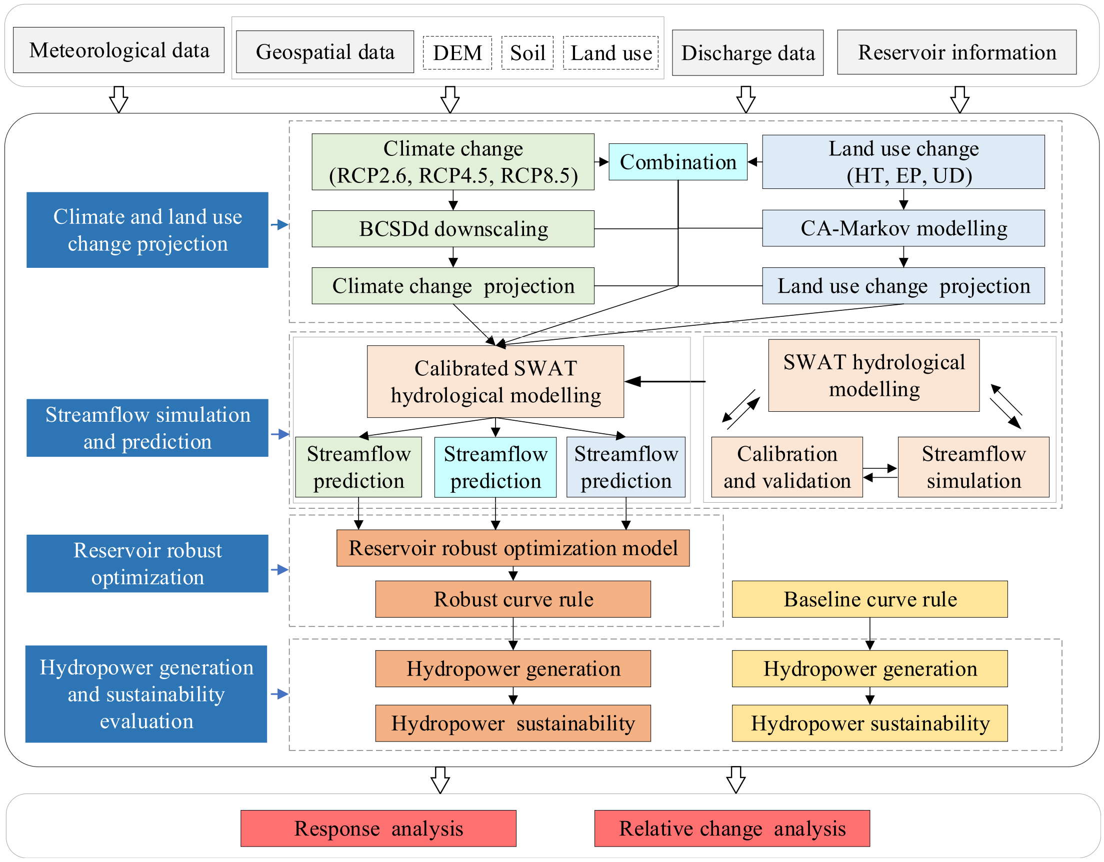

Fig. 2. Modeling framework of this study.

combined contributions of climate and land use changes on hydropower generation and sustainability. Scenarios 1–3 evaluate the future conditions under climate change (RCP2.6, RCP4.5, and RCP8.5), and Scenarios 4–6 evaluate the conditions under land use change (HT, EP, and UD). Scenarios 7–15 consider combined conditions, where RCPs are assembled with HT as HTs (i.e., HT2.6, HT4.5, and HT8.5); EP as EPs (i.e., EP2.6, EP4.5, and EP8.5); UD as UDs (i.e., UD2.6, UD4.5, and UD8.5).

3.2. SWAT hydrological simulation

The SWAT model has been successfully used in climate and land use change impact analysis and proved high reliability of short/long-term streamflow simulation at yearly/monthly scale (Zuo et al., 2016; Anand et al., 2018; Bhatta et al., 2019). We applied the SWAT distributed hydrological model to simulate and predict the long-term monthly inflow for Xinanjiang Reservoir. In the SWAT model, a catchment will be divided into several sub-basins and then separated into numerous hydrological response units (HRUs). The same HRU shares same land use and soil information. The flow in each HRU is further simulated according to a water budget equation. See Arnold et al. (1998) for details. To assess the goodness of SWAT model in the Xinanjiang catchment, the coefficients of determination (R^2) (Woldesenbet et al., 2017) and Nash-Sutcliffe efficiency (NSE) (Dile et al., 2016) are adopted in this study.

3.3. Reservoir robust optimization model formulation

In addition to the baseline operating rule, optimization schemes reasonably utilizing water resources to operate a reservoir for the sole purpose of hydropower generation are also widely applied in the field of water resources management (Fang et al., 2018). To maximize hydropower generation, we first use a reservoir optimization rule model.

$$f = \max\left(\sum_{t=1}^{T} N_t \Delta t\right) \tag{1}$$

$$N_t = AH_t Q_t^p \Delta t \tag{2}$$

where A is the power output coefficient of the hydropower plant, H_t is the tth hydraulic head (m), Q_t^p is the tth reservoir release for hydropower generation (m^3/s), N_t is the tth power output (MW), and t is the index of time step.

The operation model is subject to the following constraints:

$$\text{C1} \; V_{t+1} = V_t + \left(Q_t^i - Q_t^r\right) \times \Delta t - I_t \tag{3}$$

$$\text{C2} \; Z_{t,\min} \le Z_t \le Z_{t,\max} \tag{4}$$

$$\text{C3} \; Q_{t,\min}^r \le Q_t^r \le Q_{t,\max}^r \tag{5}$$

$$\text{C4} \; Q_{t,\min}^p \le Q_t^p \le Q_{t,\max}^p \tag{6}$$

$$\text{C5} \; N_{t,\min} \le N_t \le N_{t,\max} \tag{7}$$

$$C6d_t^{k-1} \le d_t^k \tag{8}$$

where C1-6 represent the constraints of water balance, reservoir storage, total release, turbine release, power output and operation lines, respectively; Q_t^i is the tth reservoir inflow (m^3/s), Q_t^r is the total release of reservoir (m^3/s), I_t is the tth water loss (m^3), V_t is the tth reservoir storage t (m^3), Z_t is the tth water level of reservoir (m), min and $m$ax are the top and bottom limitations, respectively; and d_t^k is the tth point of guiding curve line k (m), here the number of guiding curves is 4.

Climate and land use changes and the corresponding uncertainty may cause reservoir inflow changes, which will disrupt the consistency of hydrological data time series of the hydropower plants. To assess the vulnerability of reservoir operations to the potential uncertainties in streamflow, the objective in Eq. (1) is instead evaluated over a number of inflows under varying climate and land use changes. The uncertainties are then mitigated using a minimax approach formulated in Eq. (9), which minimizes the objectives in the worst-case realization. This approach identifying robust operating policies has been adopted in Kasprzyk et al. (2012) to improve the robustness of the identified solutions under uncertainty.

$$J = \max\min_i \left(\sum_{t=1}^{T} N_{i,t} \Delta t \right) \tag{9}$$

where $N_{i,t}$ is the tth power output under scenario i (MW).

The robust optimization model uses the uncertain inflows as the inputs under 15 climate and land use change scenarios in the future. Then the model is run with a monthly time-step and solved by Genetic Algorithm (GA).

3.4. Performance indicators

We assess the performance of different reservoir policies using indicators of sustainability and efficiency (Tian et al., 2018). The sustainability is generally determined by indicators of reliability, resilience, and vulnerability. The reliability represents the probability of the hydropower system operating satisfyingly (quantified by the power assurance rate (PAR)); the resiliency defines the ability of the hydropower plant recovering from a failure to a success status (quantified by the resiliency index (RI)); and the vulnerability measures the severity of a failure (quantified by the maximum output gap (MOG)). In this study, a failure occurs when the power output is below the firm output. The efficiency is the ability to effectively use water for electricity production and is quantified by the amount of spilled water (SW) and the water use rate (WUA). These metrics can be calculated based on equations 10–14.

$$PAR = \frac{n_{N \ge N_{base}}}{T} \times 100\% \tag{10}$$

$$RI = \frac{\sum_{t=1}^{T-1} (N_t < N_{base}) \odot (N_{t+1} \ge N_{base})}{n_{N<N_{base}}} \times 100\% \tag{11}$$

$$MOG = \max(N_{base} - N_t) \tag{12}$$

$$SW = \sum_{t=1}^{T} \max(0, Q^r - Q^p) \times 2.63/100 \tag{13}$$

$$WUA = \frac{Q^p}{Q^r} \times 100\% \tag{14}$$

where N_{base} is the firm power output (MW), $n_{N<N_{base}}$ is the number of failure states while $n_{N \ge N_{base}}$ is on the contrary, and $\odot$ is a function that returns 1 when the condition is satisfied and returns 0 otherwise. Note that the larger the PAR, RI, and WUA values are, the better the results, whereas low MOG and SW values are preferable.

4. Results

4.1. Climate and land use change projections

The mean annual temperature in 1976–2005 in the Xinanjiang catchment is 16.83 °C. In 2021–2050, the multi-model ensemble means all projects warming under RCPs, and the mean annual temperature increases by 0.25–0.69 °C with increasing radiation intensity. In addition, there is an agreement on the direction of precipitation change. The multi-model ensemble means anticipates a positive increase in the mean annual precipitation by 44.07–45.08 mm under RCPs. Fig. 3 (a) and (b) show the projected changes in the monthly temperature and precipitation in 2021–2050, respectively. The Xinanjiang catchment has four distinct seasons in both the baseline and future periods. Additionally, there is a non-uniform distribution of mean monthly precipitation in the target region, and the precipitation in spring and summer accounts for 72.93% of the total precipitation in 1976–2005.

Seen from Fig. 3 (c), forest and grassland are the two dominant land-use types in both 1995 and 2025. The areas of forest, cultivated land and water body all decrease from 1995 to 2025 under the three land use change scenarios, and the areas of the other land use types all increase to varying degrees. Overall, the areas of forest and grassland are the largest under EP, and urban land has the lowest occupancy. In contrast, the area of urban land under UD is the largest. The land use under HT has undergone less urbanization than that under UD.

4.2. Streamflow simulation and prediction

The SWAT hydrological model was calibrated and validated in 1976–1995 and 1996–2005 on a monthly scale, respectively. The model shows very good performance with values of NSE = 0.93 and R^2 = 0.92 for the calibration period and NSE = 0.92 and R^2 = 0.90 for the validation period, as shown in Fig. 4. The model captures the low flows and most peaks, especially the highest flow peak.

We then estimated the reservoir inflow variation in 2021–2050 induced by climate change, land use change, and their combination using the calibrated SWAT model and 15 scenarios. In 2021–2050, the mean annual inflow is 339.58–354.33 m^3/s, with a variation of 1.41–5.99% compared with that in 1976–2005. The mean annual inflow does not increase positively with the increasing radiation intensity under RCPs. However, the mean annual streamflow increases positively with increasing IA. In addition, we find that the mean annual inflow under the combined climate and land use change is higher than that under climate change alone but lower than that under land use alone.

Fig. 5 shows that there is an uneven distribution of mean monthly inflow in 2021–2050 along with the observations in 1976–2005. However, the uneven distribution is improved in the future. In particular, in the flood periods from April to July, the inflow accounts for 63.59% of the total inflow in 1976–2005, whereas that in 2021–2050 ranges from 59.27 to 61.44%. There are no obvious changes in monthly streamflow among the three RCPs.

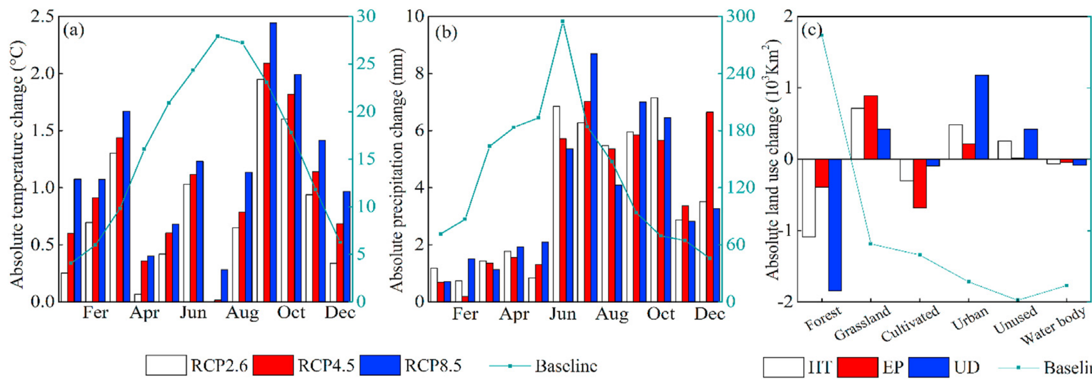

Fig. 3. Projected changes in (a) monthly precipitation, (b) monthly temperature, and (c) land use areas in the future relative to that in the baseline. The solid markers indicate the monthly precipitation and temperature, and land use areas in the baseline.

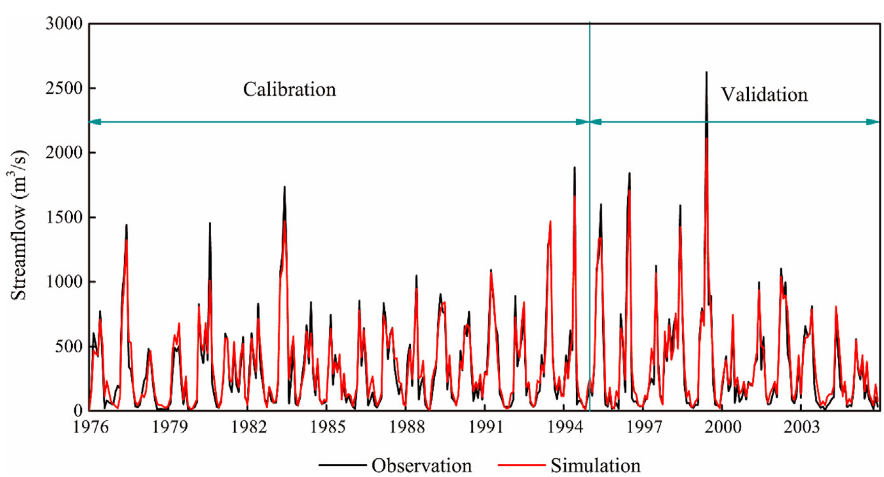

Fig. 4. Simulated and observed inflow of Xinanjiang Reservoir over the period 1976–2005.

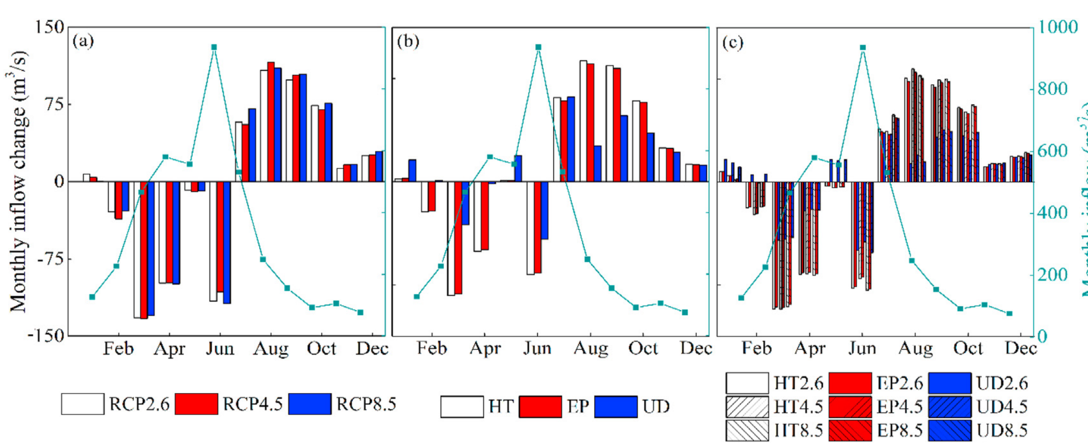

Fig. 5. Projected changes in monthly inflow under (a) climate change, (b) land use change, and (c) combined climate and land use change in 2021–2050 relative to that in 1976–2005. The solid markers indicate the monthly inflow in the baseline.

However, the monthly streamflow under UD differs from that under HT or EP. The monthly streamflow under UD from January to June is larger than that under both EP and HT, but that from August to October is smaller. And, we find that the projected changes in monthly inflow under EPs and HTs are consistent with those under RCPs alone, and that those under UDs are similar to those for UD alone. These results emphasize the complex and non-additive interactions between streamflow and climate change and land use change, and the IA greatly contributes to recharging the streamflow in the Xinanjiang catchment.

4.3. Robust rule curves with changed streamflow

The robust optimization model takes the future uncertain inflows as the inputs under 15 scenarios operated based on the monthly guiding curves within the boundary, and the results are presented in Fig. 6. Note that the region between the minimum boundary and lower curve is defined as the 0.5-times power output ($0.5N_{base}$) region, between the lower and upper curves is defined as the base power output (N_{base}) zone, between the upper and 1.5-times increased curves is defined as the 1.5-times power output region ($1.5N_{base}$), between the 1.5-times and 2.0-times increased curves is defined as the $2.0N_{base}$, and between the 2.0-times increased and maximum boundary curves is defined as the full-output (N_{full}) region. A baseline rule for Xinanjiang Reservoir that closely reproduces the dynamics of the current releases and flows is presented for comparison with the new rule. The robust curve rule differs with the baseline curve rule. Compared with that under the baseline operation rule, the lower guiding operation curve of the robust operating rule moves up in the flood seasons from January to September, and moves down in the early non-flood seasons from October to December, leading to 14.10×10^8 m^3 more useable storage in the $0.5N_{base}$ region. The upper guiding operation curve shifts upward slightly over the course of a year, and thus, the changed lower and upper guiding curves contribute to a bigger N_{base} zone. However, the 1.5-times increased output curve drops off apart from the main flood seasons from April to June, resulting in a narrower $1.5N_{base}$ region in the non-flood periods and a larger power output region in the flood periods. We find that the 2-times increased output curve declines resulting in 10.27×10^8 m^3 more useable storage in the N_{full} region from July to December due to the projected increase in inflow in the future.

4.4. Hydropower generation under changes

We simulated the historical hydropower generation with the baseline rule, and then the inflow in the future period was regulated by the baseline and robust rules, respectively. Table 3 lists the overall changes in annual hydropower generation between the periods of 2021–2050 and 1976–2005. The increase in the overall inflows reflects a continuous increase in the hydropower potential. However, the two operating rules have different effects on hydropower. The mean annual hydropower generation is 18.16×10^8 kW h/a in 1976–2005, and that in 2021–2050 shows a variation of 1.85–9.72% and 10.32–14.04% operated by the baseline and robust rules, respectively. Although the inflow varies in different land use scenarios, there are no obvious gaps among the three land use scenarios for both rules.

Fig. 7 shows the intra-annual characteristics of hydropower generation. The seasonal hydropower generation obtained with the baseline rule is sensitive to streamflow. Due to the decreased inflow from March to July, the baseline rule causes a significant decline in hydropower during the flood seasons, except under land use change alone; and an increase occurs in the non-flood seasons under all scenarios due to the increased inflow. We find an exception in February. There is a decline in reservoir inflow in February, but an increase in hydropower generation. This result is because the increased inflow from August to January contributes a high pre-water level in February; consequently, hydropower operation easily falls into the full-output region. However, the robust rule performs better than the baseline rule for hydropower outputs, and the results are less affected by streamflow with lower decreases in hydropower generation during the flood seasons from April to May and larger increments in the non-flood seasons. Additionally, the maximum increase in hydropower generation is detected in February with the baseline rule, but in August with the robust rule. The reason for this difference is that the significant inflow increase in July promotes water impoundment and a high reservoir level, thereby contributing to a larger power output. Besides, the highest power generation occurs in the flood seasons under all scenarios with the robust rule, but with the baseline rule, this is only the case for the scenarios considering rapid urbanization. These findings demonstrate that the baseline rule may not be suitable for potential future states and that a new rule is urgently needed.

4.5. Hydropower sustainability and efficiency under changes

The future overall changes in the sustainability and efficiency indicators are shown in Table 4. The reservoir system performs better in the future relative to that in the baseline period. No significant differences can be observed between the two rules regarding potential system sustainability. The PAR in 1976–2005 is 92.81%, and that in 2021–2050 generally increases and even

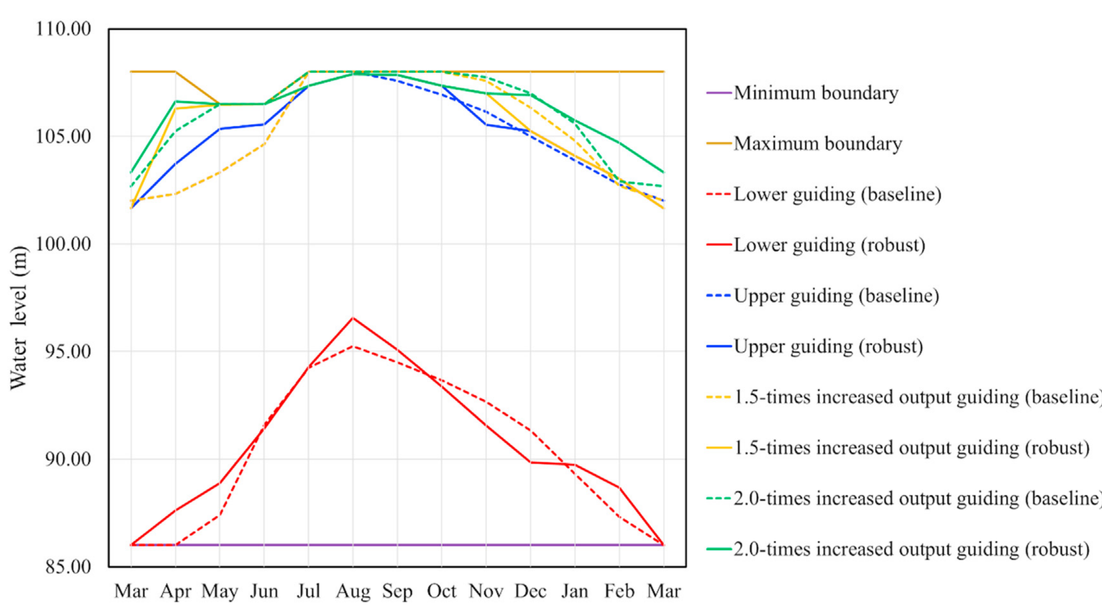

Fig. 6. Comparison between the robust and baseline operating rule.

Table 3
Overall changes in hydropower generation between 2021-2050 and 1976−2005.

Scenario	Policy		Scenario	Policy		Scenario	Policy	
	Baseline	Robust		Baseline	Robust		Baseline	Robust
RCP2.6	0.34	1.98	ED	1.62	2.27	EP4.5	1.09	2.37
RCP4.5	0.75	2.28	HT2.6	0.54	1.87	UD4.5	1.77	2.55
RCP8.5	0.76	2.29	EP2.6	0.49	2.11	HT8.5	0.86	1.98
HT	1.04	2.35	UD2.6	1.23	2.38	EP8.5	0.78	2.20
EP	1.13	2.32	HT4.5	1.33	2.17	UD8.5	0.94	2.45

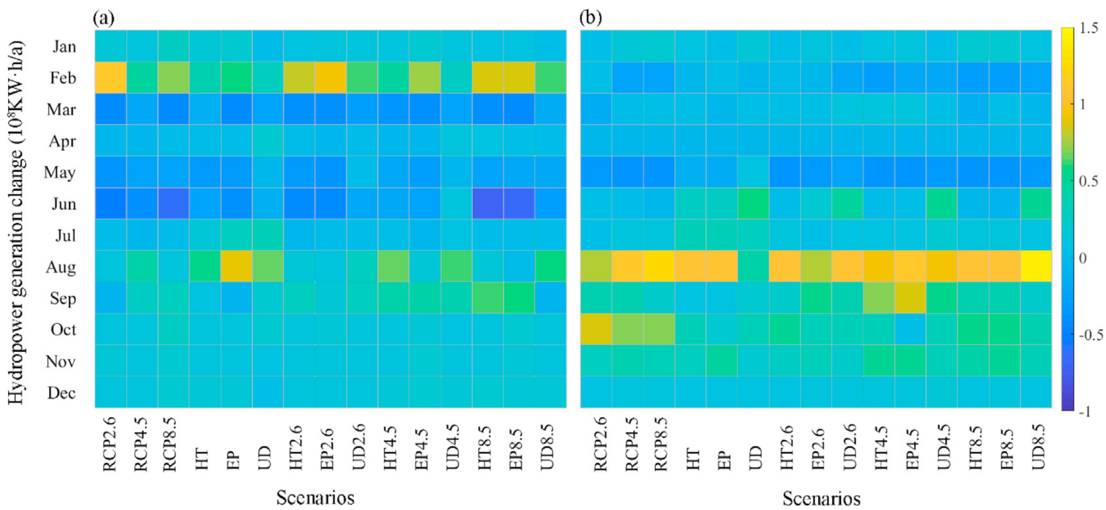

Fig. 7. Monthly changes in hydropower generation attributed to the (a) baseline and (b) robust operating rules in 2021−2050 relative to that in 1976−2005. The color of markers indicates the monthly changes in hydropower generation. (For interpretation of the references to color in this figure legend, the reader is referred to the Web version of this article.)

reaches 100%, reflecting a higher reliability to maintain the firm output attributed to both baseline and robust operating rules. The decreased MOG also indicates the lower vulnerability to output failure in the future. The RI shows relatively less obvious changes, but the trends are generally consistent with those of the AR and MOG. Especially for the robust operating rule, the reservoir system only fails to obtain the base output under land use change alone but quickly returns to a satisfactory state, with the RI equal to 1.

The increase in reservoir inflows over the whole year does not lead to an increase in SW due to the decreases in reservoir inflows during the flood seasons. However, we note that there is a significant difference on system efficiency between the two rules. It is evident that the robust rule notably improves the ability to use water for electricity production compared to the baseline rule. For the robust rule, the reservoir system performs worse under land use change alone than that under climate change alone and combination. This is because the robust optimization considers a worst-case optimization. The maximum inflow under land use change alone rarely results in a minimum hydropower generation; thus, no worst-case conditions are likely to occur. If we only consider the

Table 4
Overall changes in sustainability and efficiency indicators between 2021-2050 and 1976−2005.

Scenario	Sustainability						Efficiency			
	PAR (%)		RI		MOG (MW)		SW (108 m^3/a)		WUA (%)	
	Baseline	Robust	Baseline	Robust	Baseline	Robust	Baseline	Robust	Baseline	Robust
RCP2.6	7.18	7.18	–	–	−8.61	−8.61	−0.22	−7.17	1.08	17.27
RCP4.5	5.75	7.18	0.16	–	0.00	−8.61	−3.63	−8.00	9.03	19.03
RCP8.5	7.18	7.18	–	–	−8.61	−8.61	−2.09	−8.00	5.67	19.03
HT	5.46	6.90	0.23	0.56	0.00	−0.10	−1.30	−5.40	4.54	11.97
EP	6.61	6.90	0.56	0.56	0.00	−0.10	−2.00	−5.40	6.07	11.96
UD	6.61	5.46	0.56	0.06	0.00	−0.10	−1.76	−5.05	5.19	11.70
HT2.6	7.18	7.18	–	–	−8.61	−8.61	−1.29	−6.37	2.97	15.55
EP2.6	7.18	7.18	–	–	−8.61	−8.61	−1.35	−7.17	3.99	17.28
UD2.6	7.18	7.18	–	–	−8.61	−8.61	−2.19	−7.12	5.98	17.26
HT4.5	7.18	7.18	–	–	−8.61	−8.61	−4.41	−7.22	10.80	17.33
EP4.5	7.18	7.18	–	–	−8.61	−8.61	−3.04	−8.00	7.55	19.03
UD4.5	7.18	7.18	–	–	−8.61	−8.61	−4.22	−7.00	10.78	17.17
HT8.5	7.18	7.18	–	–	−8.61	−8.61	−2.25	−6.39	5.88	15.58
EP8.5	7.18	7.18	–	–	−8.61	−8.61	−2.29	−7.12	5.91	17.24
UD8.5	7.18	7.18	–	–	−8.61	−8.61	−1.38	−6.85	5.34	17.04

Note: The symbol "-" indicates that no failure occurs during the entire operation period.

optimization in an individual scenario, the system efficiency could be potentially maximized (SW = 0 m^3/a and WUA = 100%).

Fig. 8 shows the monthly variations in the sustainability indicators. The RI is not shown at a monthly scale because it requires a continuous sequence. Note that the monthly system sustainability is not sensitive to the operating rules. For both rules, the PAR reaches 100% and MOG reaches 0 with increasing inflow under almost all scenarios. We find that insufficient hydropower outputs mainly occur from July to November in the baseline. An abundant inflow supply in the future overcomes these shortages, and thus, the reliability and vulnerability largely improve during this period. There are some power output failures from June to September under land use change alone for both policies. This result might be caused by some lower monthly pre-water levels. For example, an insufficient output can be observed in August 2026 with a pre-water level of 94.94 m, and thereby resulting in a $0.5N_{base}$ zone.

Fig. 9 illustrates the intra-annual variation patterns of the efficiency indicators. The efficiency results are contrary to those of sustainability in the baseline hydropower simulation. There is almost no SW, indicating the full utilization of water resources for electricity production from July to December. However, easily meeting the larger power output demand (normally equal to N_{full}) results in a larger SW and a lower WUA in February and March. In addition, the WUA in June is lower than 50%, demonstrating that the baseline operation without optimization fails to effectively utilize water resources in the flood seasons. This potentially bad situation can be mitigated in the future, except those for only land use change under both policies. The reason for this exception is the same as described above and related to the output failure under land use change alone.

5. Discussion

5.1. Response analysis

Results showed that hydropower generation would increase with increasing reservoir inflows in the future. Similar results have been obtained by Wang et al. (2019b) and Zhong et al. (2020), who evaluated the hydropower generation variation induced by climate change under RCPs on the Nanliujiang River basin and the upper Yangtze River basin, China, respectively. Moreover, we found that hydropower generation was sensitive to climate change as the increase trend under RCP8.5 was the largest and more obvious than that under RCP2.6, which was also reported by Zhong et al. (2020). However, Wang et al. (2019b) demonstrated a different conclusion that RCP4.5 would generate more hydropower than other two scenarios in future. Accordingly, the extent to which hydropower generation responds to climate change varies between catchments and between scenarios. To better manage water resources and increase hydropower generation, it is essential to accurately assess future changes within a specific catchment under diverse conditions.

Fig. 10 shows the responses of annual and monthly hydropower generation to streamflow. Notably, the annual hydropower change

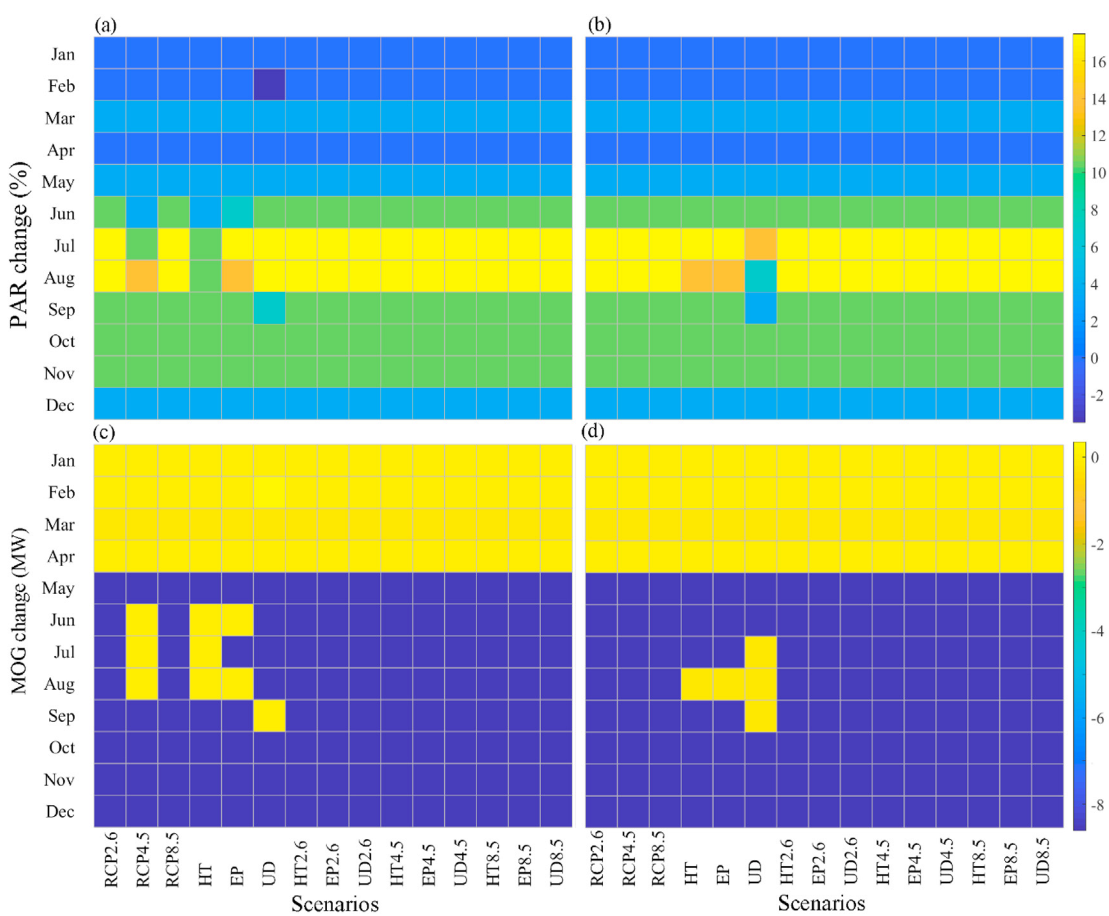

Fig. 8. Monthly changes in the PAR attributed to the (a) baseline and (b) robust operating rules, and the MOG attributed to (c) baseline and (d) robust operating rules in 2021–2050 relative to that in 1976–2005. The color of markers indicates the monthly changes in the sustainability indicators. (For interpretation of the references to color in this figure legend, the reader is referred to the Web version of this article.)

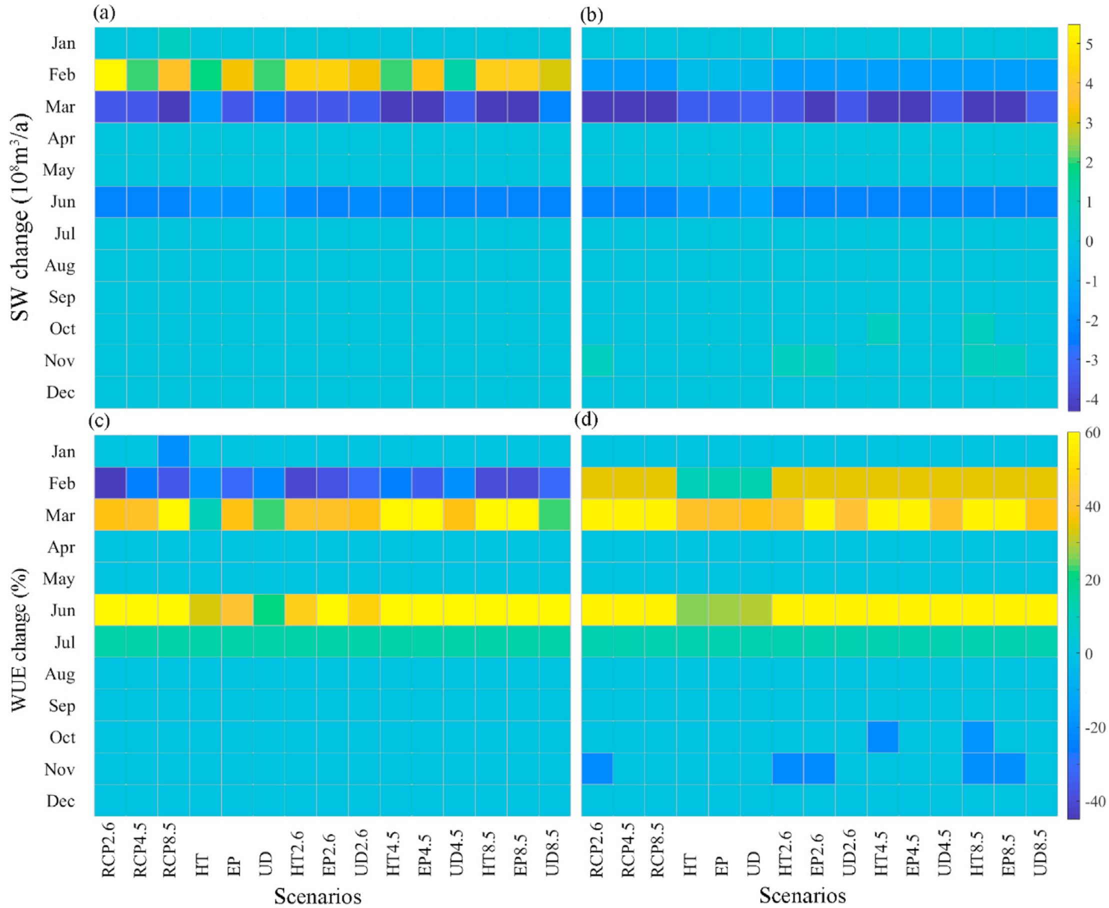

Fig. 9. Monthly changes in the SW attributed to the (a) baseline and (b) robust operating rule, and the WUA attributed to the (c) baseline and (d) robust operating rules in 2021–2050 relative to that in 1976–2005. The color of markers indicates the monthly changes in the efficiency indicators. (For interpretation of the references to color in this figure legend, the reader is referred to the Web version of this article.)

associated with the annual inflow change plots near the 1:1 line under the baseline operating rule, whereas that under the robust operating rule the plot is generally higher than the 1:1 line. This result demonstrates that the robust rule performs better in water resource utilization. To strengthen the above analysis, we find that when the monthly inflow is 20% higher in 2021–2050 to that in 1976–2005, hydropower generation is lower than the 1:1 line attributed to the baseline rule. However, hydropower generation still exists above the 1:1 line for the robust rule. In addition, for the baseline rule, at both the annual and monthly sales, the hydropower change associated with the inflow change under land use change alone is more concentrated at 0 point that under the other scenarios. This result suggests that the baseline rule would underestimate the power generation in the wet periods. However, this pattern will be broken by considering the robust optimization under uncertainty, and the mean power generation will improve by 3.72–6.83%.

Considering the complexity of hydropower computation, a narrow focus has been kept on the river discharge modelling but simplify the calculation of hydropower generation when projecting hydropower generation. For example, many previous studies assumed a linear relationship between hydropower generation and streamflow (Bartos and Chester, 2015; Kao et al., 2015; Turner et al., 2017a). These studies calculated the hydropower production based on a power output equation with a constant hydraulic head, and their hydropower generation is often referred to as the hydropower potential in the future. However, the hydropower potential was often smaller than practical hydropower generation and a comprehensive method of considering various factors should be proposed to assess the hydropower generation in the future (Wang et al., 2019b). Unlike previous studies, we not only assessed the potential changes in hydropower generation and sustainability but also provided robust operating rules for handling uncertainty attributed to both climate and land use changes. The comprehensive comparisons between the baseline and the robust rules indicated that the policy determined according to the historical hydrology condition might be no longer applicable in the future. New reservoir policy considering optimization and uncertainty is urgently needed to adapt to future potential changes, and thus to improve water resource utilization and hydropower generation. In our study, the responses of hydropower generation to streamflow were expected to be non-linear according to the above analysis. This was because we used real operating rules to regulate the inflow. A non-linear relationship could also be found in Qin et al. (2019), who considered the objective of flood control in the operation of Three George Reservoirs. Overall, our study provides a valuable reference for further hydropower assessments.

5.2. Relative change analysis

However, to directly separate the impacts of climate and land use change on hydrological regime or hydropower is almost impossible (Wang et al., 2019a). The relative change rate (RCA) (Wen et al., 2018) is defined as the ratio of changes in the output

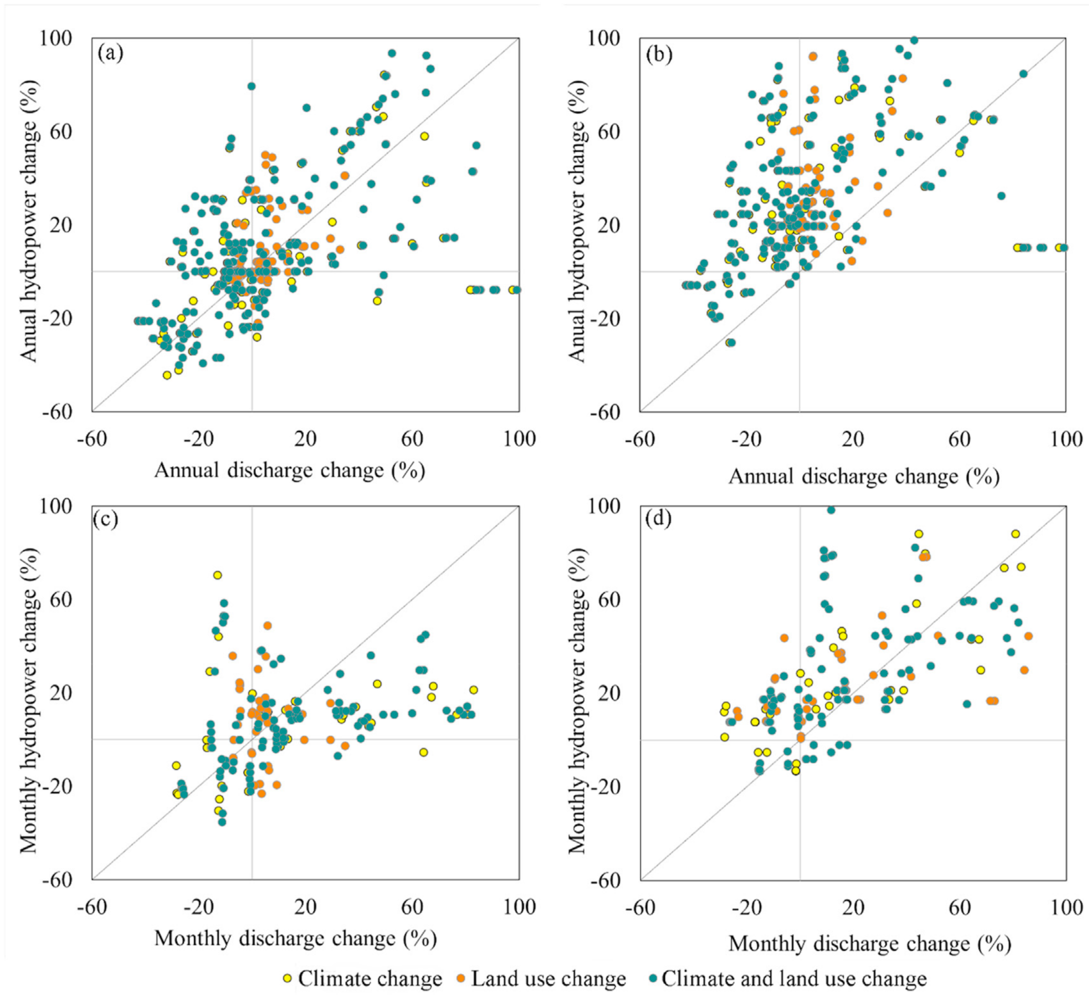

Fig. 10. Response of (a) annual and (c) monthly change in hydropower generation to inflow change attributed to baseline operating rule in 2021–2050 relative to that in 1976–2005. Response of (b) annual and (d) monthly change attributed to robust operating rule.

variable before and after considering influence factors to the standard deviation of the natural output variable, which is able to quantify the individual and combined effects of climate change and land use change on streamflow and hydropower generation in this study. See more derails for RCA in the supplemental material.

We first implemented RCA to the identify the impacts of climate and land use change on inflow. The RCA of inflow is referred to the changes in monthly inflow between 2021-2050 and 1976–2005 to the standard deviation of inflow in 1976–2005, as shown in Fig. 11 (a). The streamflow is mainly concentrated from May to July, and it is less affected by climate change relative to that in the non-flood seasons from September to October, and thus has a lower RCA, generally <0.3. This result was also noted by Wang et al. (2019c) and Wen et al. (2018), who evaluated the streamflow variation induced by climate change under RCPs in Southeast China. We find that streamflow induced by HT and EP has greater variability than UD because the strong demand for urban land under UD. In this case, the UD scenario has undergoing similar urbanization changes along with changes from 1995 to 2025. Additionally, the combined influences of climate and land use change on monthly streamflow are sensitive to the IA, climate change is the dominant factor when IA is lower under HT and EP, and the land use change is more dominant when IA is larger under UD.

Then we analyzed the individual and combined contributions of climate and land use change to hydropower generation. The RCA of hydropower is the ratio of the changes in monthly hydropower generation between 2021-2050 and 1976–2005 to the standard deviation of hydropower generation in 1976–2005. The results obtained for the baseline and robust rules are shown in Fig. 11 (b) and (c), respectively. A comparison of the certain pattern of RCA on streamflow between scenarios shows that there is no significant difference on hydropower corresponding to the non-linear relationship between streamflow and hydropower. Although the inflow in the wet periods from March to July accounts for the total inflow declines, we detect no greater difference on hydropower. For the baseline rule, the non-flood seasons from October to February have the larger RCA with increasing hydropower in the future. For the robust rule, the maximum RCA in September and November is positively affected by the increase in inflow. The above analysis of hydropower demonstrates increase in the effectiveness of water resource utilization in the future, especially for the robust operating rule associated with optimization and uncertainty.

6. Conclusions

In this study, we proposed an integrated and systematic framework to assess the potential changes in hydropower generation, sustainability and efficiency induced by reservoir policy, climate and land use change under uncertainty, using Xinanjiang Reservoir in China a case study. The framework combined climate

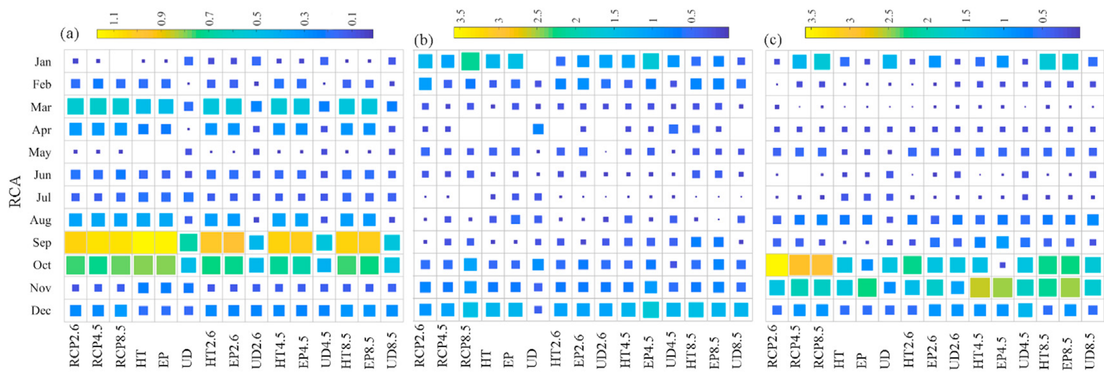

Fig. 11. Monthly RCA of (a) inflow, and hydropower generation attributed to the (b) baseline and (c) robust rules in 2021–2050 under climate and land use change relative to that in 1976–2005. The size and color of markers indicate the monthly RCA. (For interpretation of the references to color in this figure legend, the reader is referred to the Web version of this article.)

and land use change projections, streamflow simulation and prediction, reservoir robust optimization, and hydropower generation and sustainability evaluation.

Five bias-corrected and downscaled GCMs and three modeled land uses were used as inputs of the calibrated SWAT model and then to predict streamflow under 15 scenarios. The mean annual inflow in 2021–2050 was 339.58–354.33 m^3/s with a variation of 1.41–5.99% in compared with that in 1976–2005. The interactions between streamflow and climate and land use changes are non-additive, and the IA greatly contributes to recharging the streamflow. Then, the varying inflows were used as inputs to the robust optimization model for the new operating rule.

The inflow in the future was regulated by the baseline and robust rules. We found the seasonal hydropower generation obtained with the baseline rule is sensitive to streamflow. However, the robust rule performs better than the baseline rule for hydropower generation, and the results are less affected by streamflow. According to the overall increases in reservoir inflows and hydropower output, the sustainability of Xinanjiang plant was generally improved with higher PAR, higher RI, and lower MOG, in particular with the robust rule. Correspondingly, the SW did not increase in the flood seasons, resulting in an improved WUA. These results indicated that the robust rule considering optimization and uncertainty yielded better results than the baseline rule.

The response of hydropower generation to streamflow was expected to be non-linear. For the baseline rule, at both annual and monthly sales, the hydropower change associated with the inflow change under scenarios of land use change alone was more concentrated near 0 point than that under the other scenarios. However, this pattern would be broken by considering the robust optimization under uncertainty, and the mean power generation could be improved by 3.72–6.83%. In addition to the RCA, the streamflow under the rapid urbanization scenarios differs from that under other scenarios, but there was no significant difference in hydropower among all scenarios corresponding to the non-linear relationship between streamflow and hydropower change. Our findings highlight the potential for improved water resource utilization in the future, in particular with the robust operating rule considering optimization and uncertainty, and can provide references for future hydropower planning.

There are still some limitations in this study, which need to be improved in the future study. The use of multiple GCMs can avoid the potential accidental error of a single model in projecting future precipitation and temperature. We have chosen five GCM models according to their wide applications in China's climate prediction (Wen et al., 2018; Yang et al., 2019). Results have proved that their performance in this study was also good. Nevertheless, adding more applicable GCMs models may further improve the reliability and stability of predictions (Zhong et al., 2020). In addition, the long-term uncertainties under future climatic, land use and/or socio-economic changes lacking a consensus on their likelihoods and distributional forms, are termed "deep" uncertainties (Lempert et al., 2006). Different scenarios have been developed to describe the uncertainty in our study, which are far from deep uncertainty. One direction of the future study will explore scenario discovery and strategy identify under deep uncertainty (Giuliani and Castelletti, 2016; Quinn et al., 2017).

CRediT authorship contribution statement

Yuxue Guo: Conceptualization, Methodology, Writing - original draft, preparation. **Guohua Fang:** Resources, Writing - original draft. **Yue-Ping Xu:** Writing - review & editing, Funding acquisition. **Xin Tian:** Writing - review & editing. **Jingkai Xie:** Software, Visualization.

Declaration of competing interest

The authors declare that they have no known competing financial interests or personal relationships that could have appeared to influence the work reported in this paper.

Acknowledgements

This study is funded by National Key Research and Development Plan "Inter-governmental Cooperation in International Scientific and Technological Innovation" (2016YFE0122100) and the Major Project of Zhejiang Natural Science Foundation (LZ20E090001). We would like to thank the editors and anonymous reviewers for their constructive comments and suggestions.

Appendix A. Supplementary data

Supplementary data to this article can be found online at https://doi.org/10.1016/j.jclepro.2020.124609.

References

Abera, W., Tamene, L., Abegaz, A., et al., 2019. Understanding climate and land surface changes impact on water resources using Budyko framework and remote sensing data in Ethiopia. J. Arid Environ. 167, 56–64.
Ahn, K.-H., Merwade, V., 2014. Quantifying the relative impact of climate and human activities on streamflow. J. Hydrol. 515, 257–266.
Alaoui, A., Willimann, E., Jasper, K., et al., 2014. Modelling the effects of land use and

climate changes on hydrology in the ursern valley, Switzerland. Hydrol. Process. 28 (10), 3602–3614.
Anand, J., Gosain, A.K., Khosa, R., 2018. Prediction of land use changes based on Land Change Modeler and attribution of changes in the water balance of Ganga basin to land use change using the SWAT model. Sci. Total Environ. 644, 503–519.
Arango-Aramburo, S., Turner, S.W.D., Daenzer, K., et al., 2019. Climate impacts on hydropower in Colombia: a multi-model assessment of power sector adaptation pathways. Energy Pol. 128, 179–188.
Arnold, J.G., Srinivasan, R., Muttiah, R.S., et al., 1998. Large area hydrologic modeling and assessment Part I: model development 1. J. Am. Water Resour. Assoc. 34 (1), 73–89.
Bartos, M.D., Chester, M.V., 2015. Impacts of climate change on electric power supply in the Western United States. Nat. Clim. Change 5 (8), 748–752.
Beh, E.H.Y., Zheng, F., Dandy, G.C., et al., 2017. Robust optimization of water infrastructure planning under deep uncertainty using metamodels. Environ. Model. Software 93, 92–105.
Bhatta, B., Shrestha, S., Shrestha, P.K., et al., 2019. Evaluation and application of a SWAT model to assess the climate change impact on the hydrology of the Himalayan River Basin. Catena 181, 104082.
Boehlert, B., Strzepek, K.M., Gebretsadik, Y., et al., 2016. Climate change impacts and greenhouse gas mitigation effects on U.S. hydropower generation. Appl. Energy 183, 1511–1519.
Celeste, A.B., Billib, M., 2009. Evaluation of stochastic reservoir operation optimization models. Adv. Water Resour. 32 (9), 1429–1443.
Chilkoti, V., Bolisetti, T., Balachandar, R., 2017. Climate change impact assessment on hydropower generation using multi-model climate ensemble. Renew. Energy 109, 510–517.
Culley, S., Noble, S., Yates, A., et al., 2016. A bottom-up approach to identifying the maximum operational adaptive capacity of water resource systems to a changing climate. Water Resour. Res. 52 (9), 6751–6768.
De Queiroz, A.R., Faria, V.A.D., Lima, L.M.M., et al., 2019. Hydropower revenues under the threat of climate change in Brazil. Renew. Energy 133, 873–882.
De Queiroz, A.R., Marangon Lima, L.M., Marangon Lima, J.W., et al., 2016. Climate change impacts in the energy supply of the Brazilian hydro-dominant power system. Renew. Energy 99, 379–389.
Desta, Y., Goitom, H., Aregay, G., 2019. Investigation of runoff response to land use/land cover change on the case of Aynalem catchment, North of Ethiopia. J. Afr. Earth Sci. 153, 130–143.
Dile, Y.T., Daggupati, P., George, C., et al., 2016. Introducing a new open source GIS user interface for the SWAT model. Environ. Model. Software 85, 129–138.
Falchetta, G., Gernaat, D.E.H.J., Hunt, J., et al., 2019. Hydropower dependency and climate change in sub-Saharan Africa: a nexus framework and evidence-based review. J. Clean. Prod. 231, 1399–1417.
Fang, G., Guo, Y., Wen, X., et al., 2018. Multi-objective differential evolution-chaos shuffled frog leaping Algorithm for water resources system optimization. Water Resour. Manag. 32 (12), 3835–3852.
Giuliani, M., Castelletti, A., 2016. Is robustness really robust? How different definitions of robustness impact decision-making under climate change. Climatic Change 135 (3–4), 409–424.
Giuliani, M., Herman, J.D., Castelletti, A., et al., 2014. Many-objective reservoir policy identification and refinement to reduce policy inertia and myopia in water management. Water Resour. Res. 50 (4), 3355–3377.
Guo, Y., Fang, G., Wen, X., et al., 2019. Hydrological responses and adaptive potential of cascaded reservoirs under climate change in Yuan River Basin. Nord. Hydrol 50 (1), 358–378.
Kao, S.-C., Sale, M.J., Ashfaq, M., et al., 2015. Projecting changes in annual hydropower generation using regional runoff data: an assessment of the United States federal hydropower plants. Energy 80, 239–250.
Kasprzyk, J.R., Nataraj, S., Reed, P.M., et al., 2013. Many objective robust decision making for complex environmental systems undergoing change. Environ. Model. Software 42 (2), 55–71.
Kasprzyk, J.R., Reed, P.M., Characklis, G.W., et al., 2012. Many-objective de Novo water supply portfolio planning under deep uncertainty. Environ. Model. Software 34 (6), 87–104.
Kasprzyk, J.R., Reed, P.M., Kirsch, B.R., et al., 2009. Managing population and drought risks using many-objective water portfolio planning under uncertainty. Water Resour. Res. 45 (12), 170-170.
Kim, K., Jeong, H., Ha, S., et al., 2017. Investment timing decisions in hydropower adaptation projects using climate scenarios: a case study of South Korea. J. Clean. Prod. 142, 1827–1836.
Lempert, R.J., Groves, D.G., Popper, S.W., et al., 2006. A general, analytic method for generating robust strategies and narrative scenarios, 52 (4), 514–528.
Matrosov, E.S., Woods, A.M., Harou, J.J., 2013. Robust decision making and info-gap decision theory for water resource system planning. J. Hydrol. 494, 43–58.
Mendes, C.A.B., Beluco, A., Canales, F.A., 2017. Some important uncertainties related to climate change in projections for the Brazilian hydropower expansion in the Amazon. Energy 141, 123–138.
Molina-Navarro, E., Trolle, D., Martínez-Pérez, S., et al., 2014. Hydrological and water quality impact assessment of a Mediterranean limno-reservoir under climate change and land use management scenarios. J. Hydrol. 509, 354–366.
Ning, T., Li, Z., Liu, W., 2016. Separating the impacts of climate change and land surface alteration on runoff reduction in the Jing River catchment of China. Catena 147, 80–86.
Qin, P., Xu, H., Liu, M., et al., 2019. Climate change impacts on Three Gorges Reservoir impoundment and hydropower generation. J. Hydrol. 123922.
Quinn, J.D., Reed, P.M., Keller, K., 2017. Direct policy search for robust multi-objective management of deeply uncertain socio-ecological tipping points. Environ. Model. Software 92, 125–141.
Schaeffer, R., Szklo, A.S., Pereira de Lucena, A.F., et al., 2012. Energy sector vulnerability to climate change: a review. Energy 38 (1), 1–12.
Teotónio, C., Fortes, P., Roebeling, P., et al., 2017. Assessing the impacts of climate change on hydropower generation and the power sector in Portugal: a partial equilibrium approach. Renew. Sustain. Energy Rev. 74, 788–799.
Thrasher, B., Maurer, E.P., McKellar, C., et al., 2012. Technical Note: bias correcting climate model simulated daily temperature extremes with quantile mapping. Hydrol. Earth Syst. Sci. 16 (9), 3309–3314.
Tian, X., Galelli, S., Neufville, R.d., 2018. Impact of operating rules on planning capacity expansion of urban water supply systems. Urban Water J. 1–8.
Turner, S.W.D., Hejazi, M., Kim, S.H., et al., 2017a. Climate impacts on hydropower and consequences for global electricity supply investment needs. Energy 141, 2081–2090.
Turner, S.W.D., Ng, J.Y., Galelli, S., 2017b. Examining global electricity supply vulnerability to climate change using a high-fidelity hydropower dam model. Sci. Total Environ. 590–591, 663–675.
Vonk, E., Xu, Y.P., Booij, M.J., et al., 2014. Adapting multireservoir operation to shifting patterns of water supply and demand. Water Resour. Manag. 28 (3), 625–643.
Wang, F., Duan, K., Fu, S., et al., 2019a. Partitioning climate and human contributions to changes in mean annual streamflow based on the Budyko complementary relationship in the Loess Plateau, China. Sci. Total Environ. 665, 579–590.
Wang, H., Xiao, W., Wang, Y., et al., 2019b. Assessment of the impact of climate change on hydropower potential in the Nanliujiang River basin of China. Energy 167, 950–959.
Wang, Y., Lei, X., Wen, X., et al., 2019c. Effects of damming and climatic change on the eco-hydrological system: a case study in the Yalong River, southwest China. Ecol. Indicat. 105, 663–674.
Wang, Z., Xia, J., Li, T., et al., 2016. An integrated model coupling open-channel flow, turbidity current and flow exchanges between main river and tributaries in Xiaolangdi Reservoir, China. J. Hydrol. 543, 548–561.
Wen, X., Liu, Z., Lei, X., et al., 2018. Future changes in Yuan River ecohydrology: individual and cumulative impacts of climates change and cascade hydropower development on runoff and aquatic habitat quality. Sci. Total Environ. 633, 1403–1417.
Wickramasuriya, R.C., Bregt, A.K., van Delden, H., et al., 2009. The dynamics of shifting cultivation captured in an extended Constrained Cellular Automata land use model. Ecol. Model. 220 (18), 2302–2309.
Woldesenbet, T.A., Elagib, N.A., Ribbe, L., et al., 2017. Hydrological responses to land use/cover changes in the source region of the Upper Blue Nile Basin, Ethiopia. Sci. Total Environ. 575, 724–741.
Xu, Y.P., Tung, Y.K., 2008. Decision-making in water management under uncertainty. Water Resour. Manag. 22 (5), 535–550.
Xu, Y.P., Tung, Y.K., 2009. Decision rules for water resources management under uncertainty. J. Water Resour. Plann. Manag. 135 (3), 149–159.
Yang, W., Long, D., Bai, P., 2019. Impacts of future land cover and climate changes on runoff in the mostly afforested river basin in North China. J. Hydrol. 570, 201–219.
Zhang, L., Karthikeyan, R., Bai, Z., et al., 2017. Analysis of streamflow responses to climate variability and land use change in the Loess Plateau region of China. Catena 154, 1–11.
Zhang, L., Podlasly, C., Feger, K.-H., et al., 2015. Different land management measures and climate change impacts on the runoff – a simple empirical method derived in a mesoscale catchment on the Loess Plateau. J. Arid Environ. 120, 42–50.
Zhang, X., Liu, P., Xu, C.-Y., et al., 2019. Real-time reservoir flood control operation for cascade reservoirs using a two-stage flood risk analysis method. J. Hydrol. 577, 123954.
Zhong, R., Zhao, T., He, Y., et al., 2019. Hydropower change of the water tower of Asia in 21st century: a case of the Lancang River hydropower base, upper Mekong. Energy 179, 685–696.
Zhong, W., Guo, J., Chen, L., et al., 2020. Future hydropower generation prediction of large-scale reservoirs in the upper Yangtze River basin under climate change. J. Hydrol. 588, 125013.
Zuo, D., Xu, Z., Yao, W., et al., 2016. Assessing the effects of changes in land use and climate on runoff and sediment yields from a watershed in the Loess Plateau of China. Sci. Total Environ. 544, 238–250.